

A Non-rigid Multimodal Image Registration Method Based on Particle Filter and Optical Flow

Edgar Arce-Santana, Daniel U. Campos-Delgado, and Alfonso Alba

Facultad de Ciencias, Universidad Autónoma de San Luis Potosí,
Av. Salvador Nava Mtz. S/N, Zona Universitaria, 78290,
San Luis Potosí, SLP, México
Tel.: +52 444 8262486 x 2907

arce@fciencias.uaslp.mx, ducd@fciencias.uaslp.mx, fac@fc.uaslp.mx

Abstract. Image Registration is a central task to many medical image analysis applications. In this paper, we present a novel iterative algorithm composed of two main steps: a global affine image registration based on particle filter, and a local refinement obtained from a linear optical flow approximation. The key idea is to iteratively apply these simple and robust steps to efficiently solve complex non-rigid multimodal or unimodal image registrations. Finally, we present a set of evaluation experiments demonstrating the accuracy and applicability of the method to medical images.

1 Introduction

One of the most important stages in medical image analysis is the registration (alignment) of images obtained from different sources [1], [2]. For instance, image registration is a common pre-processing stage during the development of atlases, the analysis of multiple subjects, and the study of the evolution of certain diseases or injuries. Generally speaking, image registration is the problem of finding a geometrical transformation which aligns two images. Solutions to this problem can be divided in two classes: rigid and non-rigid. Rigid image registration methods assume that a single global transformation is applied equally to each pixel in the image, reducing the problem to finding only the few parameters which describe the global transformation. While rigid or affine registration is widely used, it presents serious drawbacks when one of the images shows complex deformations with respect to the other, for example, when both images belong to different subjects. On the other hand, non-rigid (also called elastic) registration methods estimate a transformation for each pixel, incorporating only weaker smoothness assumptions in order to make the problem well-posed. These methods are more general than rigid methods; however, they are also more computationally demanding, and difficult to implement and calibrate. An extensive and comprehensive survey can be found in [3], [4].

Registration methods can also be classified as unimodal, where it is assumed that pixel intensities between both images are similar, and multimodal, which

are capable of aligning images coming from different types of sensors (e.g., MRI and PET), or with inhomogeneous illumination and contrast. The most popular multimodal registration methods are based on the maximization of the mutual information (MI) between both images, a method which was originally proposed by Viola and Wells [5], and also by Collignon and Maes [6]. These methods, however, were originally described for rigid transformations; hence, recent research has mostly focused on multimodal elastic registration [7], [8], [9], [10]. Most of these methods deal with two difficulties: (1) find a model for the joint probability between both images (e.g., Parzen windows), which is required for the computation of the MI, and (2), propose an optimization algorithm (usually a complex one) capable of dealing with the non-linearities of the MI when expressed in terms of the joint probability model. Other approaches use landmarks and radial basis functions (RBF) to model local deformations as in [11], which require to detect some characteristic as edges and evaluate RBF.

A recent work [12] proposes a very different approach for MI-based rigid registration methods: instead of modeling the MI with a differentiable function (so that it can be optimized with continuous methods), a stochastic search is performed, where the MI is simply seen as a measure of similarity for each solution in a relatively large population. In this case, the authors employ a technique called Particle Filter (PF), which is commonly used for parameter estimation in dynamical systems. This new approach results in a simple yet robust method to perform multimodal affine registration with great accuracy.

This work builds from [12] to present a new approach to solve the non-rigid image registration problem. The key idea behind the proposed method lies in a two-step iterative algorithm, where we first compute the global affine registration between both images (using the PF approach), and then refine this transformation locally for each pixel using a very simple optical flow approximation. The aligned candidate image is then used as the input candidate image in the following iteration until convergence is reached. This iterative process produces a multi-stage algorithm where each stage is efficient, and easy to implement and tune, yet powerful enough to achieve complex non-rigid unimodal and multimodal registrations. The paper is organized as follows: Section 2 describes the methodology and some mathematical properties; Section 3 demonstrates the methods through some experiments and results; and finally, in Section 4, our conclusions are presented.

2 Methodology

This section describes the proposed algorithm in detail, and provides some mathematical insight about the convergence of the method. For the rest of this paper, we will use the following notation: $I_1(\mathbf{x})$ and $I_2(\mathbf{x})$ are, respectively, the reference and candidate images, both of which are observed in a finite rectangular lattice $L = \{\mathbf{x} = (x, y)\}$. For simplicity's sake, we will only deal with the 2D case, but the method can be easily extended to 3D volumes. The problem consists in finding a smooth transformation field $T_{\mathbf{x}}$ that aligns I_2 with I_1 , i.e., so that

$\tilde{I}_2(\mathbf{x}) = I_1(\mathbf{x})$ where $\tilde{I}_2(\mathbf{x}) = f(I_2(T_{\mathbf{x}}(\mathbf{x})))$, and f is an unknown tone transfer function. Here we propose a solution based on a two-step iterative approach where, at each iteration t , a high-precision affine registration technique is used to find a global transformation matrix $M^{(t)}$, and then an efficient optical flow algorithm is applied to refine the transformation locally for each pixel; specifically, the desired transformation $T_{\mathbf{x}}^{(t)}$ is obtained as

$$T_{\mathbf{x}}^{(t)}(\mathbf{x}) = M^{(t)}\mathbf{x} + \mathbf{v}^{(t)}(\mathbf{x}), \quad (1)$$

where $\mathbf{v}^{(t)}$ is the optical flow field.

This method is generalized to the multimodal case by using Mutual Information (MI) as similarity function during the affine registration stage. Once the affine transformation is found, an adequate tone transfer function $f^{(t)}$ is applied to match the grayscale levels between both images, so that the optical flow constraint holds.

Our method can be summarized in the following steps:

1. Let $t = 0$.
2. Initialize $I_2^{(0)}$ with the candidate image I_2 .
3. Find an affine transformation matrix $M^{(t)}$ that aligns $I_2^{(t)}$ with I_1 using a (possibly multimodal) affine registration method.
4. Estimate $\hat{I}_2(\mathbf{x}) = I_2^{(t)}(M^{(t)}\mathbf{x})$ using, for instance, bicubic interpolation.
5. Find a pixel-wise tone transfer function $f^{(t)}$ that adequately maps gray levels in I_1 to their corresponding gray values in \hat{I}_2 . Let $\tilde{I}_2 = f(\hat{I}_2)$.
6. Estimate the optical flow field $\mathbf{v}^{(t)}$ between I_1 and $\tilde{I}_2(\mathbf{x})$.
7. Obtain $I_2^{(t+1)}(\mathbf{x})$ as $I_2^{(t)}(M^{(t)}\mathbf{x} + \mathbf{v}^{(t)}(\mathbf{x}))$.
8. Increase t and go back to step 3 until a convergence criteria is met.

Steps 3, 5, and 6 are described below in more detail.

2.1 Algorithm Details

The key idea behind the proposed method is to efficiently perform a complex elastic registration from simple and robust building blocks, which can be tested, tuned, and optimized independently. Each particular block has been chosen to achieve a good balance between simplicity, efficiency, and accuracy. Here we discuss some of our particular choices.

Affine registration by particle filter: Registration methods based on MI have proven to be very robust for both uni-modal and multi-modal applications. One difficulty, however, is that the inherently non-linear definition of the MI results in algorithms which often require complex optimization techniques which are either computationally expensive (e.g., Markov Chain Monte Carlo (MCMC) methods), or sensitive to the initial parameters (e.g., gradient descent methods). A recent approach, introduced in [12], employs instead a stochastic search known as Particle Filter (PF) [13] to estimate the optimal parameters of the affine transformation. An overview of this algorithm is as follows:

1. Generate a random initial population $S^1 = \{s_j^1\}$ of N_s parameter vectors (particles). We specifically use seven affine parameters: rotation angle, scaling along X and Y, translation along X and Y, and shearing along X and Y.
2. Let $k = 1$. Follow the next steps until convergence is met:
 - (a) For each particle $s_j^k \in S^k$, compute the *likelihood* function $\gamma(s_j^k | I_1, \hat{I}_2)$, which in this case is given by

$$\gamma(s | I_1, \hat{I}_2) = \frac{1}{\sqrt{2\pi}\sigma} \exp \left\{ -\frac{\left(H(I_1) - \text{MI}(I_1, \hat{I}_2) \right)^2}{2\sigma^2} \right\}, \quad (2)$$

where $H(I_1)$ is the entropy of I_1 , $\text{MI}(I_1, \hat{I}_2)$ is the MI between I_1 and \hat{I}_2 , and $\hat{I}_2(x) = I_2(M_s x)$, with M_s the transformation matrix defined by parameter vector s .

- (b) Normalize the likelihoods to obtain the weights $w_j^k = \gamma(s_j^k | I_1, \hat{I}_2)/Z$, where $Z = \sum_j \gamma(s_j^k | I_1, \hat{I}_2)$, so that $\sum_j w_j^k = 1$. Note that w^k can now be seen as a distribution over S^k .
- (c) Obtain an intermediate population \hat{S}^k by resampling from population S^k with distribution w^k [13].
- (d) Generate the next population S^{k+1} by stochastically altering each particle in the intermediate population. In this case, each particle follows a random walk profile given by:

$$s_j^{k+1} = \hat{s}_j^k + \nu_j \quad j = 1, \dots, N_s, \quad (3)$$

where $\hat{s}_j^k \in \hat{S}^k$, and $\nu_j \sim \mathcal{N}(0, \Sigma^k)$; here, Σ^k is a diagonal matrix of standard deviations of the noise applied to each parameter. To enforce convergence, we apply simulated annealing to Σ^k by letting $\Sigma^{k+1} = \beta \Sigma^k$ at each iteration with $0 < \beta < 1$.

- (e) Increase k .

3. Based on the normalized weights $\{w^k\}$ for the last population, obtain the final parameter estimators s^* as the population average: $s^* = \sum_j w_j^k s_j^k$.

Some of the advantages of the PF approach are: (1) it allows complex and non-linear likelihood functions to be used, without seriously affecting the complexity of the method, (2) it is robust to its initial parameters, and (3) it can be easily generalized to the 3D case.

Estimation of tonal transfer function: Once the global transformation matrix M is known, optical flow can be used to refine the transformation at each pixel in order to achieve an elastic registration. In the multi-modal case, however, the brightness consistency constraint (also known as optical flow constraint) [14] may be violated, preventing the optical flow algorithm to estimate the correct displacements. To deal with this obstacle, one may choose an adequate tone

transfer function $f(i)$ to match the gray levels between image I_1 and the registered candidate $\hat{I}_2(\mathbf{x}) = I_2(M\mathbf{x})$. In particular, we compute $f(i)$ as a maximum likelihood estimator from the joint gray-level histogram of I_1 and \hat{I}_2 , given by

$$h_{i,j} = \sum_{\mathbf{x} \in L} \delta(I_1(\mathbf{x}) - i) \delta(\hat{I}_2(\mathbf{x}) - j), \quad (4)$$

where δ is the Kronecker delta function. The tone transfer function is thus computed as

$$f(j) = \arg \max_i p(I_1(\mathbf{x}) = i \mid \hat{I}_2(\mathbf{x}) = j) \approx \arg \max_j \{h_{i,j}\}. \quad (5)$$

Note, however, than in the unimodal case, it is possible that the estimated transfer function differs significantly from the identity, introducing spurious correlations which may affect the performance of the optical flow estimation method. When the input data is known to be unimodal, we suggest to simply use the identity function.

Optical flow estimation: Our approach for optical flow estimation is based on a discrete reformulation of the classical Horn-Schunck method [14]. Consider a first order Taylor expansion of $\tilde{I}_2(\mathbf{x} + \mathbf{v}(\mathbf{x}))$ around \mathbf{x} :

$$\tilde{I}_2(\mathbf{x} + \mathbf{v}(\mathbf{x})) \approx \tilde{I}_2(\mathbf{x}) + \nabla_{\mathbf{x}} \tilde{I}_2(\mathbf{x}) \mathbf{v}'(\mathbf{x}), \quad (6)$$

where \mathbf{v}' denotes the transpose of \mathbf{v} , so that one can write the optical flow constrain as

$$I_1(\mathbf{x}) = \tilde{I}_2(\mathbf{x}) + \nabla_{\mathbf{x}} \tilde{I}_2(\mathbf{x}) \mathbf{v}'(\mathbf{x}). \quad (7)$$

Equation 7 is ill-posed; therefore, additional regularization constraints must be introduced to obtain a unique solution. Both constraints are typically expressed by means of an energy function $U(\mathbf{v})$ that must be minimized. For efficiency reasons, we chose a quadratic penalty function for both constraints, so that $U(\mathbf{v})$ is given by

$$U(\mathbf{v}) = \sum_{\mathbf{x} \in L} \left\| \nabla_{\mathbf{x}} \tilde{I}_2(\mathbf{x}) \mathbf{v}'(\mathbf{x}) + \tilde{I}_2(\mathbf{x}) - I_1(\mathbf{x}) \right\|^2 + \lambda \sum_{\langle \mathbf{x}, \mathbf{y} \rangle} \|\mathbf{v}(\mathbf{y}) - \mathbf{v}(\mathbf{x})\|^2, \quad (8)$$

where the sum in the second term ranges over all nearest-neighbor sites $\langle \mathbf{x}, \mathbf{y} \rangle$ in L , and λ is a regularization parameter which controls the smoothness of the resulting flow field. The gradient in the first term is computed by applying an isotropic Gaussian filter to \hat{I}_2 and computing the symmetric derivatives with the kernel $(0.5, 0, -0.5)$.

Since $U(\mathbf{v})$ is quadratic in the unknowns, it can be solved very efficiently by the Gauss-Seidel method [15].

2.2 Mathematical Properties of the Problem Formulation

In general, from its proposed formulation, the nonlinear transformation field $T_{\mathbf{x}}$ that aligns I_2 with I_1 is sought under the following optimality condition

$$\max_{T_{\mathbf{x}}} \text{MI}(I_1(\mathbf{x}), I_2(T_{\mathbf{x}}(\mathbf{x}))). \quad (9)$$

This previous formulation has important robustness properties and capability to handle multimodal registration. However, the optimization problem in (9) is highly nonlinear and its solution involves a complex multivariable search. Hence, as it was mentioned at the beginning of this section, the transformation field $T_{\mathbf{x}}$ is assumed with the special structure in (1). Furthermore, it is considered that the optical flow field $\mathbf{v}^{(t)}$ can be represented as a linear combination of unknown vector fields $\hat{\mathbf{v}}^{(j)}$ $j = 1, \dots, N$, i.e.

$$\mathbf{v}^{(t)}(\mathbf{x}) = \sum_{j=1}^N \alpha^j \hat{\mathbf{v}}^{(j)}(\mathbf{x}) \quad \alpha^j \in \mathbb{R}, \forall j. \quad (10)$$

Therefore, in order to solve (9), an iterative algorithm is proposed to construct $T_{\mathbf{x}}^{(t)}$:

$$T_{\mathbf{x}}^{(t)}(\mathbf{x}) = \mathbf{M}^{(t)} T_{\mathbf{x}}^{(t-1)}(\mathbf{x}) + \mathbf{v}^{(t)}(\mathbf{x}) \quad t = 1, 2, \dots \quad (11)$$

Let us assume that $T_{\mathbf{x}}^{(-1)}(\mathbf{x}) = \mathbf{x}$, then it is satisfied in the iterative process

$$T_{\mathbf{x}}^{(1)}(\mathbf{x}) = \mathbf{M}^{(1)} \mathbf{x} + \mathbf{v}^{(1)}(\mathbf{x}) \quad (12)$$

$$T_{\mathbf{x}}^{(2)}(\mathbf{x}) = \mathbf{M}^{(2)} T_{\mathbf{x}}^{(1)}(\mathbf{x}) + \mathbf{v}^{(2)}(\mathbf{x}) \quad (13)$$

\vdots

$$T_{\mathbf{x}}^{(t)}(\mathbf{x}) = \underbrace{\left[\prod_{j=1}^t \mathbf{M}^{(t-j+1)} \right]}_{\mathbf{M}^{(t)}} \mathbf{x} + \underbrace{\sum_{j=1}^t \left[\prod_{i=1}^{t-j} \mathbf{M}^{(t-i+1)} \right]}_{\alpha^j(t) \hat{\mathbf{v}}^{(j)}(\mathbf{x})} \mathbf{v}^{(j)}(\mathbf{x}) \quad (14)$$

where $\prod_{i=a}^b \mathbf{M}^{(i)} = \mathbf{M}^{(b)} \mathbf{M}^{(b-1)} \dots \mathbf{M}^{(a)}$ for $a \leq b$, and $\prod_{i=a}^b \mathbf{M}^{(i)} = \mathbf{I}$ for $a > b$. Therefore, at t -th iteration, the resulting transformation field $T_{\mathbf{x}}^{(t)}(\mathbf{x})$ has the structure highlighted in (1) and (10). In addition, note that the iterative construction of $T_{\mathbf{x}}(\mathbf{x})$ in (11) can be interpreted as the response of a linear time-varying system under the input vector field $\mathbf{v}^{(t)}(\mathbf{x})$. Consequently, in order to guarantee the convergence (*stable response*) of (11) [16], it is sufficient to satisfy

$$\mathbf{M}^{(t)} \rightarrow \mathbf{I} \quad \& \quad \mathbf{v}^{(t)} \rightarrow \mathbf{0}, \quad \text{as } t \rightarrow \infty \quad (15)$$

where \mathbf{I} denotes the identity matrix and $\mathbf{0}$ the zero matrix, in order to guarantee

$$\|\mathbf{M}^{(t)}\| \leq \gamma \quad \forall t \quad (16)$$

and $\gamma > 0$. Therefore, we may define as convergence conditions:

$$\|\mathbf{M}^{(t)} - \mathbf{I}\| < \epsilon_1 \quad \& \quad \|\mathbf{v}^{(t)}(\mathbf{x})\| < \epsilon_2, \quad (17)$$

given $\epsilon_1, \epsilon_2 > 0$.

Hence the proposed algorithm suggests to solve iteratively the two-stage optimization problems:

I.- The rigid transformation $\mathbf{M}^{(t)}$ through the optimization process

$$J_1^{(t)} = \max_{\mathbf{M}^{(t)}} \text{MI} \left(I_1(\mathbf{x}), I_2 \left(\mathbf{M}^{(t)} T_{\mathbf{x}}^{(t-1)}(\mathbf{x}) \right) \right). \quad (18)$$

II.- And the linear optical flow $\mathbf{v}^{(t)}(\mathbf{x})$ by the following minimization problem

$$J_2^{(t)} = \min_{\mathbf{v}^{(t)}(\mathbf{x})} \sum_{\mathbf{x} \in L} \left\| \nabla_{\mathbf{x}} \tilde{I}_2 \left(\mathbf{M}^{(t)} T_{\mathbf{x}}^{(t-1)}(\mathbf{x}) \right) \mathbf{v}'^{(t)}(\mathbf{x}) + \tilde{I}_2(\mathbf{M}^{(t)} T_{\mathbf{x}}^{(t-1)}(\mathbf{x})) - I_1(\mathbf{x}) \right\|^2 + \lambda \sum_{\langle \mathbf{x}, \mathbf{y} \rangle} \left\| \mathbf{v}^{(t)}(\mathbf{y}) - \mathbf{v}^{(t)}(\mathbf{x}) \right\|^2. \quad (19)$$

Note that if $\{J_1^{(t)}\}$ and $\{J_2^{(t)}\}$ represent increasing and decreasing convergent sequences with respect to t , respectively, then conditions in (15) will be satisfied, since there is a continuity property of the parameters of $T_{\mathbf{x}}^{(t)}(\mathbf{x})$ with respect to the cost functions in the optimization processes.

Assume that the iterative algorithm stops at $t = N$, then the optimal (*locally*) transformation is given by

$$T_{\mathbf{x}}^*(\mathbf{x}) = \mathbf{M}^* \mathbf{x} + \mathbf{v}^*(\mathbf{x}) \quad (20)$$

where

$$\mathbf{M}^* = \prod_{j=1}^N \mathbf{M}^{(N-j+1)} \quad (21)$$

$$\mathbf{v}^*(\mathbf{x}) = \sum_{j=1}^N \left[\prod_{i=1}^{N-j} \mathbf{M}^{(N-i+1)} \right] \mathbf{v}^{(j)}(\mathbf{x}), \quad (22)$$

which are carried out by the method proposed here.

3 Results

In this section, we present two different kinds of results. The first one corresponds to the registration of images having similar gray values, so that the transfer function $f(\cdot)$ (see Section 2) is the identity. These kinds of experiments are important in the medical field, since for example tumors or vital organs may be monitored. Rows in Fig. 1 show a set of TC-images, these rows correspond to the

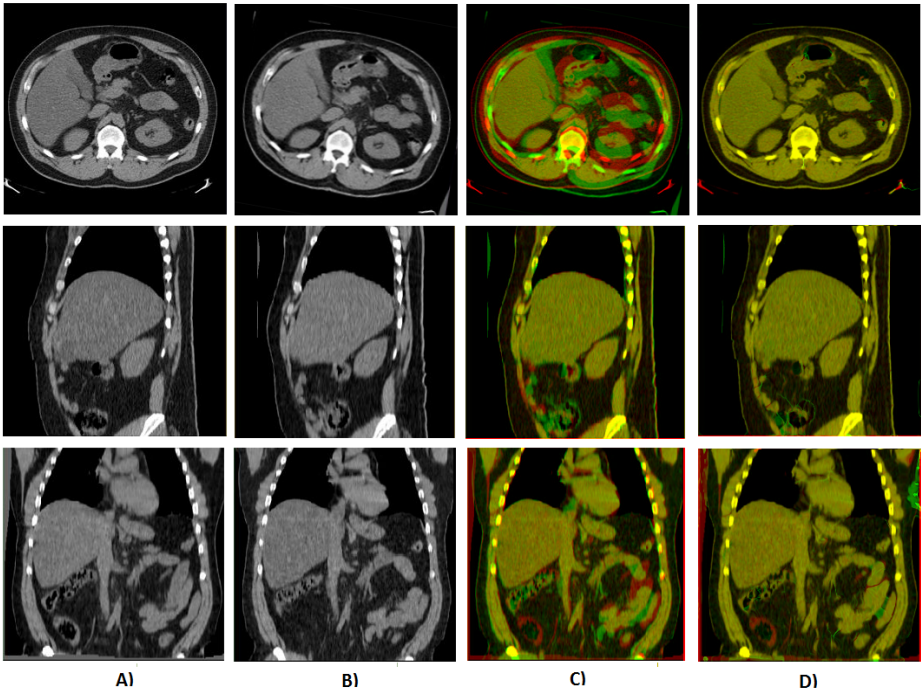


Fig. 1. Chest TC-images: *A)* Reference Image; *B)* Moving Image; *C)* Superimposed Non-registered Images; *D)* Superimposed Registered Images

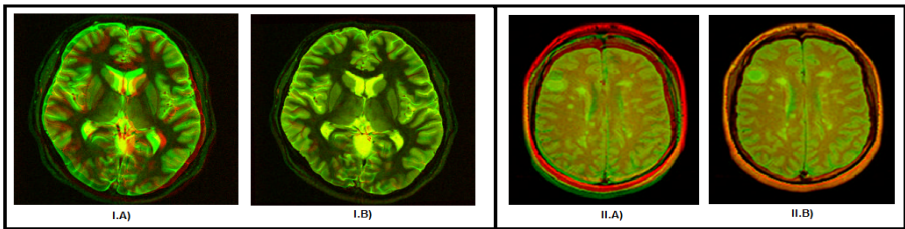


Fig. 2. Superimposed image registration: *I.A)* MRI-images before registration; *I.B)* MRI-images after registration; *II.A)* T1-GdDTPA and T2-images before registration; *II.B)* T1-GdDTPA and T2-images after registration

axial, sagittal, and coronal views from the chest of the same subject. The images in column *A)* are the reference; meanwhile, column *B)* shows the moving images. The difference between these two columns corresponds to posture and breathing in two different intervals of time. We can see in the superimposed images in column *C)* the difference between the images to register; the reference image is displayed using the red channel, while the moving image uses the green channel;

therefore, those pixels where the images coincide should look yellow. Column D) shows the non-rigid image registration obtained by the proposed method. Notice how some structures have been deformed in order to achieve a good matching, reducing the pixels in red or green, and incrementing the matching pixels in yellow explained by a good elastic registration; the image size (in pixels) for the axial, sagittal, and coronal views are respectively 247×242 , 268×242 , and 268×244 ; and the registration times were 214, 231, and 231 seconds. All the these experiments were performed on a PC running at 3.06 GHz.

The following set of experiments concern to the case of multimodal image registration. Panel I in Fig. 2 shows the registration of anatomical (spin-echo) MRI images of two different subjects; observe how the different structures in the center of the Fig. 2-I.A) are aligned after the registration (2-I.B)). Similar results are shown in Panel II in Fig 2, which corresponds to the alignment of a T1-weighted MRI-image, with a contrast agent (gadolinium diethylene triamine pentaacetic acid), with a T2-weighted image from the same subject.

In all the experiments described above , we used the same set of parameters; the values of the main parameters are defined in Table 1.

Table 1. Main parameter values of the non-rigid registration algorithm

Particle Filter						
Particles	Likelihood- σ	PF-Iterations	Displacement- σ	Angle- σ	Scale- σ	Shearing- σ
200	$H(I_1)/6$	150	2	0.2	0.02	0.02
Optical Flow						
Iterations		λ		Smoothing- σ		
200		2000		0.5		

4 Conclusions

We presented a new iterative algorithm which is mainly based on two building blocks: 1) a global affine registration, and 2) a linear optical flow. The key idea behind this approach is to efficiently perform a complex elastic registration from these simple and robust building blocks. The affine registration was carried out by an accurate algorithm based on the particle filter [12], meanwhile the second block can be solved very efficiently by a Gauss-Seidel method. We provided the mathematical properties which support the problem formulation, and establish some convergence conditions. Finally, we presented experiments where the algorithm proved to be efficient, and accurate to estimate complex 2D elastic unimodal and multimodal registrations.

Acknowledgements. This work was supported by grant PROMEP/UASLP/-10/CA06.

References

1. Hajnal, J., Hawkes, D., Hill, D.: Medical image registration. CRC, Boca Raton (2001)
2. Modersitzki, J.: Numerical Methods for Image Registration. Oxford University Press, Oxford (2004)
3. Zitova, B., Flusser, J.: Image registration methods: a survey. *Image and Vision Computing* 21, 977–1000 (2003)
4. Brown, L.G.: A survey of image registration techniques. *ACM Computing Survey* 24, 326–376 (1992)
5. Wells III, W.M., Viola, P.A., Atsumi, H., Nakajima, S., Kikinis, R.: Multi-modal volume registration by maximization of mutual information. *Medical Image Analysis* 1, 35–51 (1996)
6. Maes, F., Collignon, A., Vandermeulen, D., Marchal, G., Suetens, P.: Multimodality image registration by maximization of mutual information. *IEEE Trans. Med. Image.* 16, 187–198 (1997)
7. Zhang, J., Rangarajan, A.: Bayesian Multimodality Non-rigid image registration via conditional density estimation. In: Taylor, C.J., Noble, J.A. (eds.) IPMI 2003. LNCS, vol. 2732, pp. 499–512. Springer, Heidelberg (2003)
8. Periaswamy, S., Farid, H.: Medical image registration with partial data. *Medical Image Analysis* 10, 452–464 (2006)
9. Arce-Santana, E., Alba, A.: Image registration using markov random coefficient and geometric transformation fields. *Pattern Recognition* 42, 1660–1671 (2009)
10. Bagci, U., Bai, L.: Multiresolution elastic medical image registration in standard intensity scale. *Computer Graphics and Image Processing* 29, 305–312 (2007)
11. Yang, X., Zhang, Z., Zhou, P.: Local elastic registration of multimodal image using robust point matching and compact support RBF. In: International Conference on BioMedical Engineering and Informatic, BMEI-(2008)
12. Arce-Santana, E., Campos-Delgado, D.U., Alba, A.: ISVC 2009. LNCS, vol. 5875, pp. 554–563. Springer, Heidelberg (2009)
13. Arulampalam, M.S., Maskell, S., Gordon, N., Clapp, T.: A Tutorial on Particle Filters for Online Nonlinear/Non-Gaussian Bayesian Tracking. *IEEE Transactions On Signal Processing* 50, 174–188 (2002)
14. Horn, B.K.P., Schunck, B.G.: Determining Optical Flow. *Artificial Intelligence* 17, 185–203 (1981)
15. Barrett, R., Berry, M., Chan, T.F., Demmel, J., Donato, J., Dongarra, J., Eijkhout, V., Pozo, R., Romine, C., van der Vorst, H.: *Templates for the Solution of Linear Systems: Building Blocks for Iterative Methods*, 2nd edn. SIAM, Philadelphia (1994)
16. Rugh, W.J.: *Linear System Theory*. Prentice-Hall, Englewood Cliffs (1996)